



HAL
open science

Heat recovery from Diesel engines: a thermodynamic comparison between Kalina and ORC cycles

Paola Bombarda, Costante Invernizzi, Claudio Pietra

► **To cite this version:**

Paola Bombarda, Costante Invernizzi, Claudio Pietra. Heat recovery from Diesel engines: a thermodynamic comparison between Kalina and ORC cycles. *Applied Thermal Engineering*, 2009, 30 (2-3), pp.212. 10.1016/j.applthermaleng.2009.08.006 . hal-00521157

HAL Id: hal-00521157

<https://hal.science/hal-00521157>

Submitted on 26 Sep 2010

HAL is a multi-disciplinary open access archive for the deposit and dissemination of scientific research documents, whether they are published or not. The documents may come from teaching and research institutions in France or abroad, or from public or private research centers.

L'archive ouverte pluridisciplinaire **HAL**, est destinée au dépôt et à la diffusion de documents scientifiques de niveau recherche, publiés ou non, émanant des établissements d'enseignement et de recherche français ou étrangers, des laboratoires publics ou privés.

Accepted Manuscript

Heat recovery from Diesel engines: a thermodynamic comparison between Kalina and ORC cycles

Paola Bombarda, Costante Invernizzi, Claudio Pietra

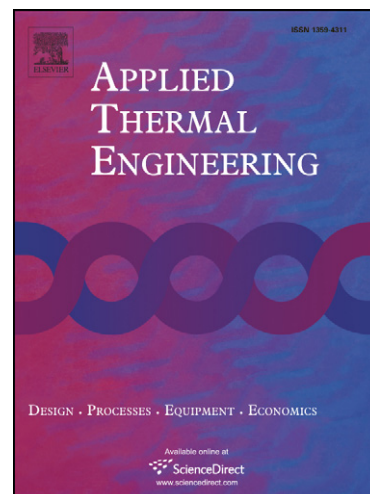
PII: S1359-4311(09)00251-8
DOI: [10.1016/j.applthermaleng.2009.08.006](https://doi.org/10.1016/j.applthermaleng.2009.08.006)
Reference: ATE 2875

To appear in: *Applied Thermal Engineering*

Received Date: 14 April 2009
Revised Date: 25 May 2009
Accepted Date: 14 August 2009

Please cite this article as: P. Bombarda, C. Invernizzi, C. Pietra, Heat recovery from Diesel engines: a thermodynamic comparison between Kalina and ORC cycles, *Applied Thermal Engineering* (2009), doi: [10.1016/j.applthermaleng.2009.08.006](https://doi.org/10.1016/j.applthermaleng.2009.08.006)

This is a PDF file of an unedited manuscript that has been accepted for publication. As a service to our customers we are providing this early version of the manuscript. The manuscript will undergo copyediting, typesetting, and review of the resulting proof before it is published in its final form. Please note that during the production process errors may be discovered which could affect the content, and all legal disclaimers that apply to the journal pertain.



Heat recovery from Diesel engines: a
thermodynamic comparison between Kalina
and ORC cycles

Paola Bombarda * Costante Invernizzi † Claudio Pietra ‡

May 25, 2009

*Department of Energy, Politecnico of Milan, via Lambruschini 4, 20156 Milano, Italy.

E-mail address: paola.bombarda@polimi.it

†**Corresponding Author** – Department of Mechanical and Industrial Engineering, University of Brescia, Via Branze 38, 25123 Brescia, Italy. E-mail address: costante.invernizzi@unibs.it

‡Department of Mechanical and Industrial Engineering, University of Brescia, Via Branze 38, 25123 Brescia, Italy. E-mail address: claudio.pietra@unibs.it

Abstract

In the context of heat recovery for electric power generation, Kalina cycle (a thermodynamic cycle using as working fluid a mixture of water and ammonia) and Organic Rankine Cycle (ORC) represent two different eligible technologies. In this work a comparison between the thermodynamic performances of Kalina cycle and an ORC cycle, using hexamethyldisiloxane as working fluid, was conducted for the case of heat recovery from two Diesel engines, each one with an electrical power of 8900 kWe. The maximum net electric power that can be produced exploiting the heat source constituted by the exhaust gases mass flow (35 kg/s for both engines, at 346 °C) was calculated for the two thermodynamic cycles. Owing to the relatively low useful power, for the Kalina cycle a relatively simple plant layout was assumed. Supposing reasonable design parameters and a logarithmic mean temperature difference in the heat recovery exchanger of 50 °C, a net electric power of 1615 kW and of 1603 kW respectively for the Kalina and for the ORC cycle was calculated.

Although the obtained useful powers are actually equal in value, the Kalina cycle requires a very high maximum pressure in order to obtain high thermodynamic performances (in our case, 100 bar against about 10 bar for the ORC cycle). So, the adoption of Kalina cycle, at least for low power level and medium-high temperature thermal

sources, seems not to be justified because the gain in performance with respect to a properly optimized ORC is very small and must be obtained with a complicated plant scheme, large surface heat exchangers and particular high pressure resistant and no-corrosion materials.

Keywords: Organic Rankine Cycles, ORC, Ammonia–Water Cycles, Kalina cycles, bottoming cycles, Diesel engines, thermodynamic conversion cycles.

Nomenclature

Symbols and acronyms

p	pressure, bar
T	(absolute) temperature, K
t	temperature, °C
R	gas constant, J/kgK
v	specific volume, m ³ /kg
ω	acentric factor of the working fluid
x	mass fraction
y	molar fraction
k_{ij}	binary interaction coefficients
a	coefficient of the Peng–Robinson equation of state, J/kg
b	coefficient of the Peng–Robinson equation of state, m ³ /kg
Λ	logarithmic mean temperature difference in heat exchangers, °C
U	global heat transfer coefficient, W/m ² K
S	heat exchanger surface, m ²
\dot{m}	mass flow, kg/s

HP high pressure

IP intermediate pressure

LP low pressure

MM acronym for hexamethyldisiloxane

ORC Organic Rankine Cycle

Subscripts

cr critical point of the working fluid

r reduced temperature and pressure ($T_r = T/T_{cr}$, $p_r = p/p_{cr}$)

sat saturated conditions

owf organic working fluid

NH₃ ammonia

1 Introduction

In many situations in the industrial world and in the energy generation field it may be convenient, or even necessary, to recover heat from a variable temperature heat source: from flue gas, for example, from the exhausts of a gas turbine or from hot gases or liquids originated by industrial processes. The electrical energy production from geothermal hot water is another typical application of sensible heat exploitation.

The use of non-azeotropic mixtures, as working fluids in Rankine cycles, has been proposed by many authors in the past years, see for example, [1, 2, 3, 4], just with the aim of reducing the thermal irreversibilities in the heat introduction process, particularly between the heat source and the evaporating working fluid.

It is exactly in this context that the Kalina cycle [5, 6] was proposed. The Kalina cycle is an absorption power cycle using ammonia-water as working fluid and it is conceptually different from the Rankine cycles working with non-azeotropic mixtures, even though the final thermodynamic aim is the same: the reduction of thermal irreversibilities obtained, first of all, by minimizing the logarithmic mean temperature difference between the heat source and the working fluid stream (having fixed the minimum pinch-point temperature difference, for example).

In comparison with the simple absorption cycle of Maloney and Robertson, as described in [7], the first version of the Kalina cycle is characterized by a second condenser, after the separator, at one intermediate pressure, allowing an additional degree of freedom in the composition of the boiling mixture and allowing the distillation unit to operate at a pressure lower than the maximum one. A further difference concerns the recuperative heat exchanger, which, in the Kalina scheme, is placed downstream the turbine.

At present, the heat recovery from high temperature gases, as in the modern combined cycles, or in multi-megawatts coal thermoelectric plants, is monopolized by the steam Rankine cycles and the more believable application of the Kalina cycle is restricted to medium-low temperatures heat sources (typical maximum temperatures of 300–400 °C in the case of heat recovery, and 100–120 °C in the binary geothermal plants) and to small power conversion systems [8, 9, 10, 11].

In these situations the plant layout may be simplified and, for example, the cycle described in [9] has a single main condenser, at the lowest cycle temperature, and the separator is placed after the evaporator.

It is specifically in the sector of the heat recovery that the Kalina cycle is in competition with the ORC cycle. The Organic Rankine Cycle is an old idea, see, for example [12, 13], and it proved to be a worthwhile tool to fulfill the thermodynamic conversion of recovered sensible heat in electrical

energy during the years. In the ORC's the proper selection of the working fluid, generally a pure fluid, which must be selected according to the source temperature level and power range, allows the best exploitation of the heat source.

In literature many works dealing with the thermodynamic performances of the Kalina cycle are available. Performance evaluation is conducted in [14], by considering the heat recovery of about 3.0 MW from a hot gas source at 550 °C, simulating gas turbine exhausts. The Author assumes a thermodynamic cycle evaporation pressure of 100 bar and an inlet turbine temperature of 500 °C. The turbine efficiency is assumed 90% and the availability of condensation water at 15 °C is also supposed. The calculated efficiency of the cycle results about 32–33%. Other works compare the performance of Kalina cycle with respect to a reference cycle. In [15] the Authors carry out an analysis on the thermodynamic advantages of using ammonia–water mixtures cycles in cogeneration plants in comparison with steam Rankine cycles, pointing out no considerable differences in the useful power for the discussed case (100 MW fuel thermal power input). In [16] the recovery from gas diesel engines is considered and many plant configurations are analysed, finding out considerable better efficiencies when compared with steam Rankine cycles assumed as reference. A comparison between Kalina and ORC performance for low temperature applications (geothermal source) is conducted in [11].

The authors compare the Kalina cycle, properly optimized as far as ammonia content and evaporation pressure are concerned, with ORC cycles which adopt either isobutane or ammonia as working fluid. The conclusions point out that better performance (calculated as net power/source mass flow) are obtainable with Kalina cycle; moreover Kalina advantage is higher in respect to isobutane ORC than ammonia ORC. As a further example, in [17] an extensive assessment on the performances of several geothermal binary plants (adopting ORC cycles) is done and the Author finds, on the basis of the Second Law efficiency, percent differences in the performance of about only few points between a reference binary cycle and the Kalina cycle operating in Húsavík, as described, for example in [9].

In this paper we consider the possibility of recovering heat from the exhaust gases of two large size Diesel engines (characterized by an electric power of 17.8 MW) by means of a Kalina cycle and by means of an ORC cycle. We assumed for the calculations a relative simple configuration for the Kalina cycle because the limited power levels of the particular considered application do not justify an excessive plant complication and we considered the net useful electrical power as the final function to be optimized.

The working fluid selected for this application of the ORC is the hexamethyldisiloxane ($((\text{CH}_3)_3\text{SiO}_{1/2}-\text{O}_{1/2}\text{Si}(\text{CH}_3)_3$, MM). Methylsiloxanes were proposed some years ago as working fluids in Rankine cycles [18] and are today

actually used in several engines [19].

2 Calculation model

The thermodynamic analysis of the considered cycles was carried out by means of a commercial software [20] aimed at calculation of complex power plants.

2.1 Thermodynamic properties of the working fluids

The thermodynamic properties of the water–ammonia mixture and of the MM were calculated using the standard Peng–Robinson equation of state, one of the many analytical equations of state available in the data bank of the adopted software:

$$p = \frac{RT}{v - b} - \frac{a}{v(v + b) + b(v - b)} \quad (1)$$

where

$$b = \sum_{i=1}^N x_i b_i$$

$$b_i = 0.07780 \frac{RT_{cr,i}}{p_{cr,i}}$$

$$a = \sum_{i=1}^N \sum_{j=1}^N x_i x_j \sqrt{a_i a_j} (1 - k_{ij})$$

$$a_i = \alpha_i(T) 0.45724 \frac{R^2 T_{cr,i}^2}{p_{cr,i}}$$

$$\alpha_i(T) = \left[1 + m_i \left(1 - \sqrt{T_{r,i}} \right) \right]^2$$

$$m_i = 0.37464 + 1.54226\omega_i - 0.26992\omega_i^2$$

$$\omega_i = -\log p_{r,sat} - 1.00 \quad \text{at} \quad T_r = 0.7$$

for ammonia–water mixtures: $N = 2$, $k_{11} = k_{22} = 0.0$, $k_{12} = k_{21} = -0.2589$; critical parameters and acentric factors are given in the **Table 1**

The equation of state was tested for the ammonia–water mixture on the data reported in [21, 22, 23, 24]. Vapour–liquid equilibrium was calculated at various pressures and temperatures, from ambient conditions up to 150 bar and about 200 °C, with maximum deviations of few percent on the equilibrium pressures and of about $\pm 15 \div \pm 20$ percent on the calculated vapour fraction for mixtures with a low contents of ammonia or water.

The thermodynamic properties (density, enthalpy and entropy) calculated by means of Equation 1 for saturated liquid and vapour along the saturated curves, resulted in a good accord with [24] for a mixture of $0.7\text{NH}_3 - 0.3\text{H}_2\text{O}$, molar fraction.

As a consequence of these tests we adopted the Equation 1 in all the following cycle simulations with ammonia–water mixtures.

For the selected working fluid of the ORC, the Equation 1 was used again, yet adapted to the case of a pure single component fluid: $N = 1$,

$k_{11} = 0.0$, $x_1 = 1.0$. The working fluid selected is MM, a linear polysiloxane of low molecular weight which is one of the main components of some silicone based heat transfer fluids. Actually no exhaustive thermodynamic data are available for MM fluid, so we tested the Equation 1 on the only experimental data available, i.e. the vapour pressures reported in [25]. In the temperature interval between 302.78 K ($T_r = 0.58$) and 383.3 K ($T_r = 0.74$) and with pressure varying from 7 mbar to 1.33 bar, the mean error on the calculated pressures was about 2 %.

Given the specific thermodynamic character of our work and in consideration of the relatively low temperature levels assumed, we will not consider corrosion aspects and thermal stability limits related to the use of the chosen working fluids. Nevertheless the known corrosion problems with ammonia-water mixtures in the generators of the absorption chillers above 200 °C with usual construction materials are to be mentioned. On the contrary silicone fluids, and therefore MM, are non corrosive in normal operating conditions towards common metals and alloys and carbon steel can be used in heat exchangers. Silicone heat transfer fluids have a recognized and accepted good thermal stability at temperatures up to about 400 °C.

Heat transfer coefficients of boiling pure ammonia are similar to that of the boiling pure water and are 10–20 times as high as those of the ordinary organic refrigerants. In the ammonia–water mixture, however, the boiling

heat transfer coefficients decrease by a third, at least in pool boiling [26]. In any case, in both gas heat exchangers of Kalina and ORC plant, the global heat transfer coefficient is dominated by the gas-side thermal resistance, and at equal US parameter it is reasonable to expect the same total surface S .

2.2 The Húsavík plant as a comparison case

Calculation model was preliminarily tested on the Húsavík plant, the first operating ammonia-water geothermal plant. In this case the variable temperature heat source has a rather low initial temperature (122 °C) and a simple plant scheme is adopted; in **Figure 1** it is represented the cycle scheme implemented for the calculation.

Assuming some reasonable design data we compared our results with those reported in [9]. The assumed turbine and pump efficiencies were respectively 0.70 and 0.58; the electrical efficiency of the motor pump was assumed 0.95 and that of the electric generator 0.96. The cycle maximum pressure, 35 bar and minimum pressure, 5.6 bar, were set so as to give together with total pressure drop, 3 bar (distributed among the heat exchangers), the proper values of evaporation and condensation pressures.

At the separator the ammonia mole fraction in the vapour and in the liquid streams resulted 97% and 49.3% against values of 95% and 50% re-

ported in [9]; the turbine gross power resulted 1823 kW matching exactly the declared value, and the pump power 132 kW (against 134 kW, [9]).

The conversion efficiency of the cycle results about 11%. As clearly highlighted in **Figure 2**, the evaporation line and the condensation of the ammonia–water mixture follows well the geothermal water (the heat source) cooling ($\Delta = 8.7$ °C) and the heating heat sink water ($\Delta = 7.8$ °C) curves. It is necessary to point out the very low temperature (5 °C) of the condensation water, hardly ever available in power plants, and the relatively low value (70%) of the turbine efficiency we had to assume to calculate the useful power, which is however consistent with the small size of the turbine.

3 Recovery heat from Diesel engines

In Diesel engines heat is available for recovery from exhaust gases, jackets, intercooler and lube oil system. In order to make the comparison between ORC and Kalina thermodynamic cycles easier, we considered as a fundamental reference case only the heat recovery from the exhaust gases, which constitutes the main item in the heat balance; it must be reminded moreover that, in all other cases, the available heat is at a much lower temperature than the exhaust gases and it is therefore not easily suitable for direct electric energy production (it could be used to boost the plant scheme in plant heat

exchangers).

The conceptual scheme of the considered system is represented in **Figure 3**, where the exhausts of two identical Diesel engines feed the heat recovery exchanger of the heat recovery cycle.

Each internal combustion engines is a Diesel Wartsila, 20V32 model, with a nominal electric power of 8900 kW at 750 rpm, and an electric efficiency of 46.0%. Exhaust gas mass flow (molar composition: 74.6 % nitrogen, 11.7 % oxygen, 6.7 % steam, 5.9 % carbon dioxide and 1.1 % argon) is 17.5 kg/s at 346 °C, which gives an available thermal power of 5730 kW (11460 kW for both engines) which could be recovered by cooling the exhausts down to the ambient temperature (assumed in this work equal to 25 °C). Low temperature heat (available from jackets at a temperature comprised between 96 - 80 °C) which is not recovered in this reference case, amounts to 5988 kW (2994 kW from every motor). Performance evaluation is conducted by assuming a direct thermal exchange between the flue gases and working fluid of the power cycle, without the adoption of any intermediate thermal heat transfer fluid. Working fluid condensation is accomplished by means of water, available at 25.0 °C and with a discharge temperature of 35 °C.

3.1 Evaluation of the Kalina cycle performance

Several plant schemes are proposed for the Kalina cycle, each one aimed at a different concern; considering the rather low power level of our application, a simple plant scheme is suggested: the plant scheme selected for this work is one of the schemes suited for high temperature heat recovery [27] and is represented in **Figure 4.a** as sketched for the calculation program.

The ammonia-water mixture has a variable composition during the cycle in order to optimize the heat introduction and heat rejection processes: mixers, separator and splitter are therefore needed to get the local requested composition, and four loop sections at different mixture composition (very rich, rich, poor and very poor, with reference to ammonia content) are detectable in the plant. The ammonia rich mixture (78.6 % molar fraction for the optimized case considered in this work) expands in *turbine* from A to B, see **Figure 4.a** and **Figure 4.b**, condenses partially at constant pressure in the *LP recuperator* and it is then mixed (*LP mixer* in the calculation scheme) with the solution very poor in ammonia (32.0 %) coming from the *separator* in order to give a composition relatively poor in ammonia (point C), suitable for the condensation process (i.e. 61.3 % in this case), which is fulfilled in the *LP condenser*. From this point, the *LP pump* brings the mixture to the separator pressure, which is intermediate between the minimum

pressure of the condenser and the maximum pressure of the heat recovery exchanger. The mixture flow, heated in *IP and LP recuperators* enters the *separator* in two phase flow condition at point D, and it is then divided in a saturated liquid flow, very poor in ammonia (point E) and a saturated vapour flow, very rich in ammonia (point F). The flow very poor in ammonia, as already discussed, is used to dilute the flow coming from the turbine before the condenser, while the very rich ammonia flow (94.9 %), is used to enrich the mixture coming from the *splitter* and finally going to the *heat recovery exchanger*. The mixture flow coming from the IP mixer (point G) is then condensed in the *IP condenser*, brought to the maximum pressure by the *feed pump* and preheated in the *HP recuperator* (point H) before being sent to the *heat recovery exchanger*; its composition will not be varied during turbine expansion and up to the LP mixer.

It is clear that, in order to calculate the plant performance, a relevant number of parameters are to be set: conventional values for the logarithmic mean temperature differences in the heat exchangers were assumed (see **Table 2**); basic assumptions for the plant components are listed in **Table 3**, together with cold source assumptions. For the sake of simplicity, pressure drops in the heat exchangers were neglected.

With the considered assumptions, the operating parameters which still need to be optimized are evaporation pressure, saturator pressure and am-

monia molar fraction during condensation and evaporation processes. Thermodynamic optimization, aimed at maximizing the plant net power, brings evaporation pressure to a very high value: however, very high pressures require high thickness for the plant components, and therefore a relevant plant cost, which is not justified for a small power plant; for this reason, and in agreement with many other authors, the evaporation pressure in this work was limited to a value as high as 100 bar.

The separator pressure has a meaningful role: its value determines the relative fraction between the outgoing liquid flow and vapor flow; a preliminary analysis showed that (see **Figure 5**, where net power is shown against evaporation ammonia molar fraction for three different values of separation pressure, p_S , (9.7 bar, 10.0 bar e 11.0 bar), in order to increase the power, a low separation pressure is desirable: a value of 10 bar was selected, as with lower values complete phase change happens in the recuperator and exiting liquid flow vanishes. The influence of the separator pressure on the plant performance is anyway not of capital interest.

The cycle was further investigated adopting the selected separation pressure of 10 bar and varying the evaporation and condensation molar fraction: results are presented in **Figure 6**, where net power is shown against evaporation molar fraction, with condensation molar fraction as a parameter. From this picture it appears that the net plant power exhibits a maximum in the

range 75-80 % of evaporation ammonia molar fraction; moreover, it is noticeable that a high ammonia molar fraction at the evaporator may be obtained only with a relevant condensation ammonia molar fraction.

On the basis of this preliminary analysis, optimum evaporation and condensation molar fractions were selected: these, together with the pressure in the separator, determine automatically molar fractions in all other points of the plant and mass fractions to be splitted or mixed.

The evaluated thermodynamic cycle efficiency is 19.7 % and net electric power is 1615 kW; exhaust gases are cooled to 127.7 °C. Detailed plant performance evaluation is presented in the **Table 4**.

From T-Q diagram (**Figure 4.b**) it is noticeable that all the low temperature heat exchangers work properly, and therefore the possible utilization of the low temperature heat, coming from the jackets, which is disregarded in this work, would not add a substantial benefit.

3.2 Evaluation of the ORC cycle performance

The considered ORC cycle is shown in **Figure 7** (plant scheme and thermodynamic cycle in the T-S plane). The working fluid, the hexamethyldisiloxane, expands in turbine from A to B and pre-heats the liquid (from E to F) coming out from the feed pump by means of a recuperative heat exchanger

(from B to C). Exhausted vapour condensation takes place between points C and point D; remaining liquid pre-heating and subsequent evaporation are fulfilled in the heat recovery exchanger from point F to A.

In order to make a sound comparison, basic assumptions already made for Kalina cycle as far as heat exchangers, turbomachinery and cold source are regarded, were maintained also for ORC cycle evaluation (see **Table 2** and **Table 3**).

In a heat recovery Rankine cycle, with given hot and cold heat sources, the only free variable which need to be optimized is the evaporation pressure p_E (or equivalently, the working fluid mass flow \dot{m}_{owf} : if the evaporation pressure gets lower, at constant temperature difference in the heat exchanger, the recovered heat will be higher and consequently a greater working fluid mass flow will be generated, but this will work in a thermodynamic cycle with a lower efficiency, thus requiring an optimization process aimed at giving the greatest power).

In **Figure 8**, it is shown the net useful power as a function of the working fluid mass flow \dot{m}_{owf} for various logarithmic mean temperature differences Λ_{HRE} in the heat recovery exchanger. The highest curve represents the reference case, with $\Lambda_{HRE} = 50$ °C. In this case (see **Table 5**) the optimum evaporation pressure is 9.7 bar, condensation pressure 0.12 bar, and the corresponding thermodynamic cycle is represented in a T-Q plane, in **Figure**

9. The thermodynamic cycle efficiency is 21.5 % and net electric power is 1603 kW; exhaust gases are cooled to 148.4 °C.

4 The comparison between Kalina and ORC cycles

The comparison between Kalina and ORC cycles is conducted at variable logarithmic mean temperature difference in the heat recovery exchanger, starting from the reference case $\Lambda_{HRE} = 50$ °C. Optimization of operating parameters for both Kalina and ORC cycle at reference case was thoroughly discussed in previous paragraphs, at variable logarithmic mean temperature difference operating parameters vary slightly, and their variation was anyway considered. As an example consider the evaporation pressure of the ORC cycle: from **Figure 8** it is noticeable that the optimum \dot{m}_{owf} changes slightly from 26 kg/s at $\Lambda_{HRE} = 50$ °C, to 25 kg/s at $\Lambda_{HRE} = 75$ °C. As already discussed, the Kalina cycle has a limit for the evaporation pressure, due to cost of components, which is fixed to 100 bar. Although limited, this pressure requires however higher than standard components: it was therefore considered interesting to investigate the cycle performance at a lower pressure (50 bar), which allows to adopt less expensive components.

In **Figure 10** it is reported the useful electrical power as a function of the logarithmic mean temperature difference in the heat recovery heat exchanger, Λ_{HRE} , for both the Kalina cycle and the ORC cycles.

Owing to the relatively high heat source temperature, the net useful power for the Kalina cycle at 50 bar is invariably smaller than the power produced by the ORC cycle of about 50–70 kW. At a maximum pressure of 100 bar the performance of the two cycles become comparable and the theoretical advantage of the Kalina cycle comes out only at Λ_{HRE} lower than 60 °C: at $\Lambda_{HRE} = 50$ °C, net power is about 1615 kW, for the Kalina and 1600 kW for ORC, while at high logarithmic mean temperature differences ($\Lambda_{HRE} = 75$ °C) the ORC prevails with 1400 kW against 1375 kW of the Kalina.

In order to have a comprehensive view of the difference between the Kalina and ORC cycles, as far as the thermodynamic performance are concerned, it is helpful to compare the thermodynamic quality of the reference recovery cycles ($\Lambda_{HRE} = 50$ °C) with respect to an ideal reversible cycle operating between the variable temperature heat source (the exhaust gas from the Diesel engines) and the ambient. Prior to proceed with calculations, it is necessary to define a reference discharge temperature for the exhausts from the heat recovery exchanger, which is set in this case at 100 °C. With this assumption, the maximum available thermal power which can be recovered from the exhausts amounts to 9258 kW; the reversible cycle efficiency amounts

to 0.3863 and for the calculated cycles, the recovery efficiency (net electric power / available thermal power) is as follows: 0.1744 for the Kalina at 100 bar, 0.1731 for the ORC, 0.168 for the Kalina at 50 bar. These figures can be understood with the aid of **Figure 11**, where all the efficiency losses are reported. The adoption of the 100 bar evaporation pressure in the Kalina cycle, allows to have a small heat recovery exchanger loss: however, this brings a relative high exhausts discharge temperature (127.7 °C) with respect to the 50 bar Kalina cycle (105.7 °C) and therefore the sum of heat recovery exchanger and reject heat losses are almost the same for both Kalina cycles, and definitely lower than the corresponding ones for the ORC cycle. The ORC cycle overcomes the heat introduction disadvantage with all the other components: the sum of the three Kalina recuperators losses is higher than the loss of the single ORC recuperator; the sum of the absorber and condenser Kalina losses is higher than the single ORC condenser loss; turbine expansion loss is again smaller for the ORC cycle and other remaining losses typical of Kalina cycle (mostly due to mixing processes) bring to a situation in which the 100 bar Kalina cycle is only slightly better than the ORC cycle, which is in turn better than the 50 bar Kalina cycle.

As a matter of fact, the heat recovery exchanger of the ORC cycle is also characterized by a lower US than the corresponding exchanger for the Kalina cycle: 150 kW/K a $\Delta_{HRE} = 50$ °C, against 165 for the Kalina at the

same Λ_{HRE} and 100 bar; being the heat exchange coefficient U almost equal for both cycles, this means that the Kalina cycle requires greater surfaces of more expensive materials. The situation is opposite if the recuperator at turbine outlet is to be considered, but it has also to be noted that the Kalina cycle has three recuperators instead of one (the same argument remains valid for the condenser).

During calculations, turbine efficiency was considered the same for both ORC and Kalina cycles: however the turbine design is as well favorable to the ORC cycle, as the isentropic enthalpy drop is definitely higher for the Kalina than ORC (575 kJ against 92 kJ for the 100 bar case). A preliminary sizing of the turbine, applying similarity rules and choosing a reasonable specific speed for axial stages (0.4) which corresponds to an isentropic efficiency slightly lower than 0.9, allows to design a single stage turbine with a rotational speed of 3000 rpm, i.e. without the need of a gear box for the ORC cycle. On the other side, the high isentropic drop suggests usually the adoption of radial stage for the Kalina cycle [28]: in order to have a good efficiency, a specific speed of 0.35 is chosen, and the rotational speed required is very high (higher than 60000 rpm), thus requiring a gear box, and adding therefore gearbox losses; as a consequence, even if the isentropic efficiency are similar, the global efficiency of the Kalina turbine should be lower than the efficiency of the ORC turbine. Moreover it has to be considered that for

the turbine, in order to avoid corrosion, titanium must be adopted [28] which is a very expensive material.

5 Conclusions

Kalina and ORC cycles for heat recovery applications in the frame of medium temperatures (typical for Diesel engine discharge) and low power levels were investigated, so as to compare their thermodynamic performance. A preliminary optimization procedure for the most important parameters was performed for both cycles prior to cycle comparison. On the basis of the calculations performed and with the assumption considered, it emerges that:

1. the Kalina cycle requires a very high maximum pressure in order to obtain high thermodynamic performance; if 50 bar maximum pressure for the Kalina cycles is selected, which is still much higher than the maximum pressure of the MM ORC cycle, low performance for the Kalina cycle is obtained;
2. if a 100 bar maximum pressure is selected for the Kalina cycle, the thermodynamic performance of both cycle are similar, and the Kalina cycle is slightly better at low logarithmic mean temperature differences in the heat recovery exchanger, i.e., the thermodynamic advantage resulting from heat introduction and heat rejection processes under very

low temperature differences is substantial only if very large heat exchange surfaces are adopted;

3. the turbine is a critical component for the high pressure Kalina cycle, which must be either multistage or rotate at very high rotational speed in order to guarantee satisfying isentropic efficiencies;
4. corrosion problems for the Kalina components, which require the adoption of expensive material, are not to be forgotten.

As a conclusion it can be said that even if the adoption of the Kalina cycle may be reasonable in the geothermal power plants, because the low temperature of the source allows the adoption of a low maximum evaporation pressure (32.3 bar, in Húsavík plant), and the Kalina cycle permit a gain in performance with respect to ORC, the adoption of Kalina cycle, at least for low power level and medium high temperatures thermal sources, seems not to be justified as the gain in performance with respect to a properly optimized ORC is very small and must be however obtained with a complicated plant scheme, large surface heat exchangers and particular high pressure resistant and no-corrosion materials, i.e., with an expensive and not proven technology.

References

- [1] B.M. Burnside, The immiscible liquid binary Rankine cycle, *Journal Mechanical Engineering Science*, 18 (2) (1976), 79–86.
- [2] M. Uematsu, K. Watanabe, N. Kagawa, Role of the thermophysical properties study of the binary refrigerant mixtures for the ORC–Technology, in *VDI Berichte 539, ORC–HP–Technology. Working fluid problems*, Proceedings of the International CDI–Seminar held in Zürich, 10–12 September 1984, pp. 99–111.
- [3] G. Angelino, P. Colonna, Multicomponent working fluids for Organic Rankine Cycles (ORCs), *Energy*, 23 (6) (1998), 449–463.
- [4] G. De Simon, D. Micheli, R. Taccani, Analisi delle prestazioni di un gruppo ORC operante con alcune miscele di polisilossani, 60-esimo Congresso Nazionale ATI Roma, Settembre 2005. Thermodynamic analysis of organic Rankine cycles operating with siloxane mixtures, Paper presented at the 60th National Congress of the Italian Association of Heat Technology, September 2005, Rome (in Italian).
- [5] A.I. Kalina, Combined cycle system with novel bottoming cycle, *ASME Journal of Engineering for gas turbine and power*, 106 (1984), 734–742.

- [6] A.I. Kalina, H.M. Leibowitz, Kalina cycle promises improved efficiency, *Modern Power System Review*, 7 (1987), 19–23.
- [7] O.M. Ibrahim, S.A. Klein, Absorption power cycles, *Energy*, 21 (1) (1996), 21–27.
- [8] M. Jonnson, J. Yan, Ammonia–water bottoming cycles: a comparison between gas engines and gas diesel engines as prime movers, *Energy*, 26 (2001), 31–44.
- [9] H. Hjartarson, R. Maack, S. Johannesson, Húsavík energy multiple use of geothermal energy, *GHC Bulletin*, June 2005, 7–13.
- [10] R. DiPippo, *Geothermal Power Plants: Principles, Applications and Case Studies*, Elsevier, Oxford UK, 2005, (Chapter 8, pag. 183, Figure 8.17).
- [11] H.D. Madhawa Hettiarachchi, M. Golubovic, W.M. Worek, Y. Ikegami, The performance of the Kalina cycle system 11 (KSC–11) with low–temperature heat sources, *Transactions of the ASME, Journal of Energy Resources Technology*, September 2007, Vol. 129, 243–247.
- [12] C. Casci, G. Angelino, P. Ferrari, M. Gaia, G. Giglioli, E. Macchi, Experimental results and economics of a small (40 kW) Organic Rankine

- Engine, 15th Intersociety Energy Conversion Engineering Conference, Seattle, Washington, August 18–22, 1980, paper 809199.
- [13] C. Invernizzi, P. Iora, P. Silva, Bottoming micro–Rankine cycles for micro–gas turbines, *Applied Thermal Engineering*, 27 (2007), 100–110.
- [14] C. H. Marston, Parametric analysis of the Kalina cycle, *ASME Journal of Engineering for Gas Turbine and Power*, 112 (1990), 107–116.
- [15] C. Dejfors, E. Thorin, G. Svedberg, Ammonia–water power cycles for direct–fired cogeneration applications, *Energy Convers. Mgmt.*, 39 (16–18) (1988), 1675–1681.
- [16] M. Jonnson, J. Yan, Exergy and pinch analysis of diesel engine bottoming cycles with ammonia–water mixtures as working fluid, *International Journal of Applied Thermodynamics*, 3 (2) (June 2000), 57–71.
- [17] R. DiPippo, Second Law assessment of binary plants generating power from low–temperature geothermal fluids, *Geothermics*, 33 (2004), 565–586.
- [18] G. Angelino, C. Invernizzi, Cyclic methylsiloxanes as working fluids for space power cycles, *Transaction of the ASME, Journal of Solar Energy Engineering*, 115, (August 1993), 130–137.

- [19] A. Duvia, M. Gaia, ORC plants for power production from biomass from 0.4 MWe to 1.5 MWe: technology, efficiency, practical experiences and economy, Paper presented at the 7th Holzenergie – Synopsium, 18 October 2002, ETH Zürich.
- [20] Aspen Plus software, 2006 version, Aspen Technology Inc., 200 Wheeler Road, Burlington, Massachusetts 01803 USA.
- [21] S.H. Rizvi, R.A. Heidemann, Vapor–liquid equilibria in the ammonia–water system, *Journal of Chemical and Engineering Data*, 32, (1987), 183–191.
- [22] T.M. Smolen, D.B. Manley, B.E. Poling, Vapor–liquid equilibrium data for the $\text{NH}_3\text{--H}_2\text{O}$ system and its description with a modified cubic equation of state, *Journal of Chemical and Engineering Data*, 36, (1991), 202–208.
- [23] R. Tillner–Roth, D.G. Friend, Survey and assesment of available measurements on thermodynamic properties of the mixture {water–ammonia}, *Journal of Physical and Chemical Reference Data*, 27 (1), (1998), 45–61.
- [24] R. Tillner–Roth, D.G. Friend, A Helmholtz free energy formulation of the thermodynamic properties of the mixture {water–ammonia}, *Jour-*

- nal of Physical and Chemical Reference Data, 27 (1), (1998), 63–96.
- [25] O.L. Flaningam, Vapour pressure of poly(dimethylsiloxane) oligomers, Journal of Chemical and engineering Data, 31 (3), (1986), 266–272.
- [26] H. Arima, M. Monde, Y. Mitsutake, Heat transfer in pool boiling of ammonia/water mixture, Heat and Mass Transfer, 39 (2003), 535–543.
- [27] P. Nag, A.V.S.S.K.S. Gupta, Exergy analysis of the Kalina cycle, Applied Thermal Engineering, 18(6), (1998), 427–439.
- [28] F. Marcuccilli, S. Zouaghi, Radial Inflow turbines for Kalina and Organic Rankine Cycles, Proceedings European Geothermal Congress 2007

Figure Captions

Figure 1 Schematic component layout of the geothermal power plant of Húsavík assumed for the calculation.

Figure 2 The Húsavík thermodynamic cycle in the T–Q (Temperature–Power) plane.

Figure 3 The conceptual scheme for the considered case of heat recovery from Diesel engines.

Figure 4 Component layout of the considered Kalina system (Figure 4.a) and the optimized thermodynamic cycle in the T–Q (Temperature–Power) plane (Figure 4.b).

Figure 5 Kalina cycle at 100 bar evaporation pressure: net power as a function of the ammonia molar fraction in the evaporator and for three pressures at the separator.

Figure 6 Kalina cycle at 100 bar evaporation pressure: net power as a function of the ammonia molar fraction in the evaporator and for three ammonia molar fractions at the low pressure condenser.

Figure 7 Hexamethyldisiloxane ORC cycle: T–S diagram and component layout.

Figure 8 Net power of the hexamethyldisiloxane ORC cycles as a function of the working fluid mass flow for various logarithmic mean temperature differences in the recovery heat exchanger.

Figure 9 Hexamethyldisiloxane ORC cycles: T-Q diagram and component layout.

Figure 10 Comparison among optimized Kalina and ORC cycles as a function of the logarithmic mean temperature difference in the heat recovery exchanger.

Figure 11 Thermodynamic efficiency losses and recovery efficiency for the optimized ORC cycle and for the optimized Kalina at 100 bar (K100) and 50 bar (K50) evaporation pressures. 1. heat recovery exchanger, 2. heat rejection, 3. recuperators, 4. condenser, 5. absorber, 6. pumps, 7. turbine, 8. mixing and valves, 9. organic and electric losses, 10. recovery efficiency.

Table 1: Thermodynamic parameters of the considered pure working fluids.

	Ammonia	MM	Water
Critical temperature, °C	133.7	245.6	374.2
Critical pressure, bar	116.0	19.14	221.0
Normal boiling point, °C	-33.3	100.5	100.0
Acentric factor ^a	0.2526	0.4152	0.3449

$${}^a\omega = -\log p_{r,sat} - 1.0, \text{ at } T_r = 0.7$$

Table 2: Values of the logarithmic mean temperature differences in the heat exchangers assumed for the calculations.

Heat exchanger	Λ , °C
Heat recovery exchanger	50
LP recuperator	15
IP recuperator	10
HP recuperated	10
Absorber	10
Condenser	10

Table 3: Assumptions for power plant components and cold source.

hydraulic pump efficiency	0.7
isoentropic turbine efficiency	0.75
mec./ electric generator efficiency	0.96
mec./ electric motor efficiency	0.95
condenser water inlet temperature, °C	25
condenser water outlet temperature , °C	35

Table 4: Calculation results for the optimized high temperature Kalina cycle.

maximum pressure, bar	100	
minimum pressure, bar	5.94	
exhausts discharge temperature, °C	127.7	
net power, kW	1615	
cycle efficiency, %	19.7	
recovery efficiency %	17.5	
	ammonia molar fraction, %	mass flow, kg/s
point A, evaporation	78.6	4.34
point E, liquid separator	32.0	2.64
point C, LP condensation	61.3	6.97
point F, vapour separator	94.9	2.21
	thermal power, kW	US , kW/K
LP recuperator	3574	238
IP recuperator	761	76.1
HP recuperator	900	90.8
LP condenser	4210	421.0
IP condenser	2309	230.9
HRE	8207	164.1

Table 5: Calculation results for the optimized high temperature ORC cycle.

maximum pressure, bar	9.74	
minimum pressure, bar	0.12	
exhausts discharge temperature, °C	148.4	
net power, kW	1603	
cycle efficiency, %	21.5	
recovery efficiency %	17.3	
	thermal power, kW	<i>US</i> , kW/K
recuperator	4444	296.3
condenser	5771	577.1.1
HRE	7445	148.9

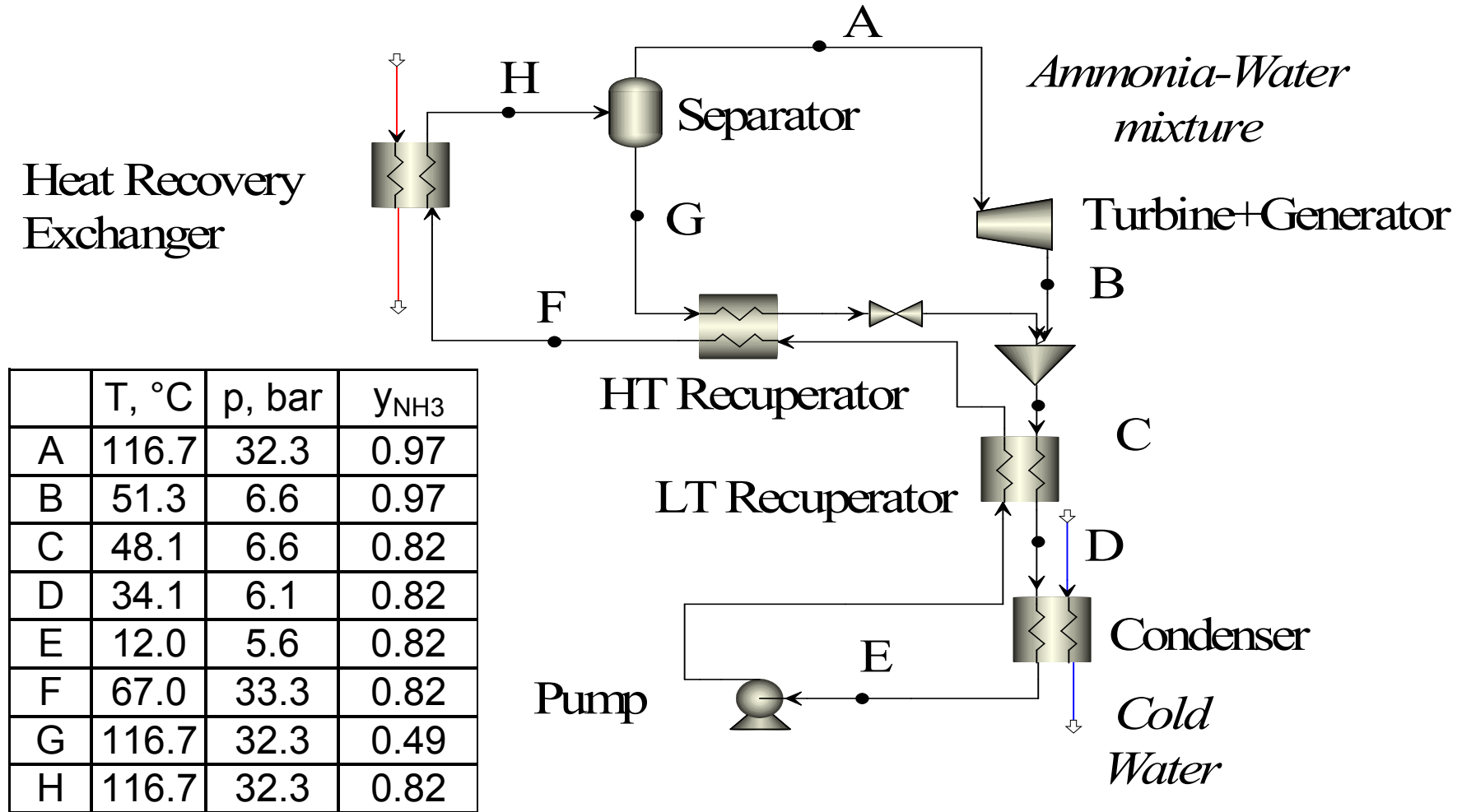
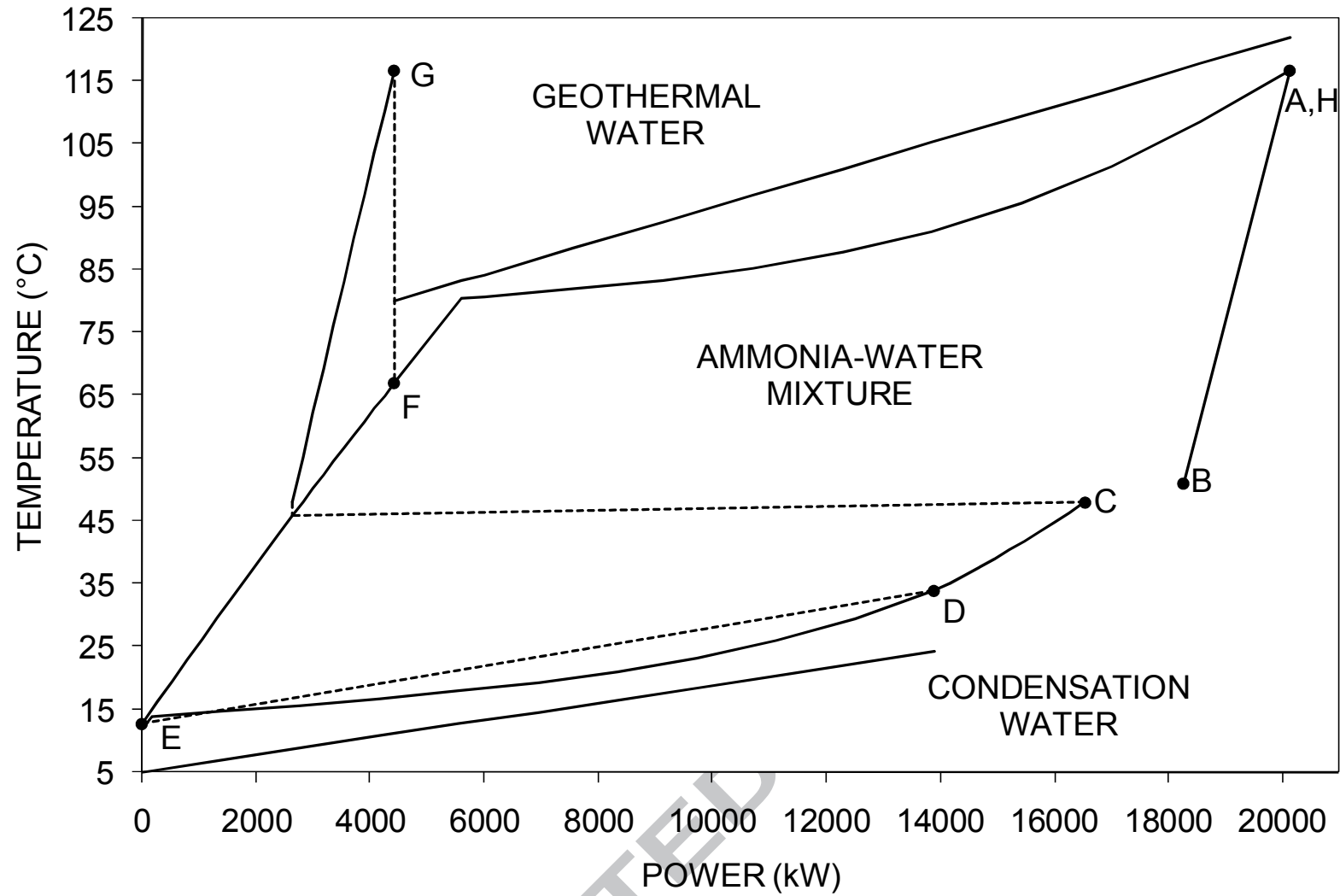


Figure 1

**Figure 2**

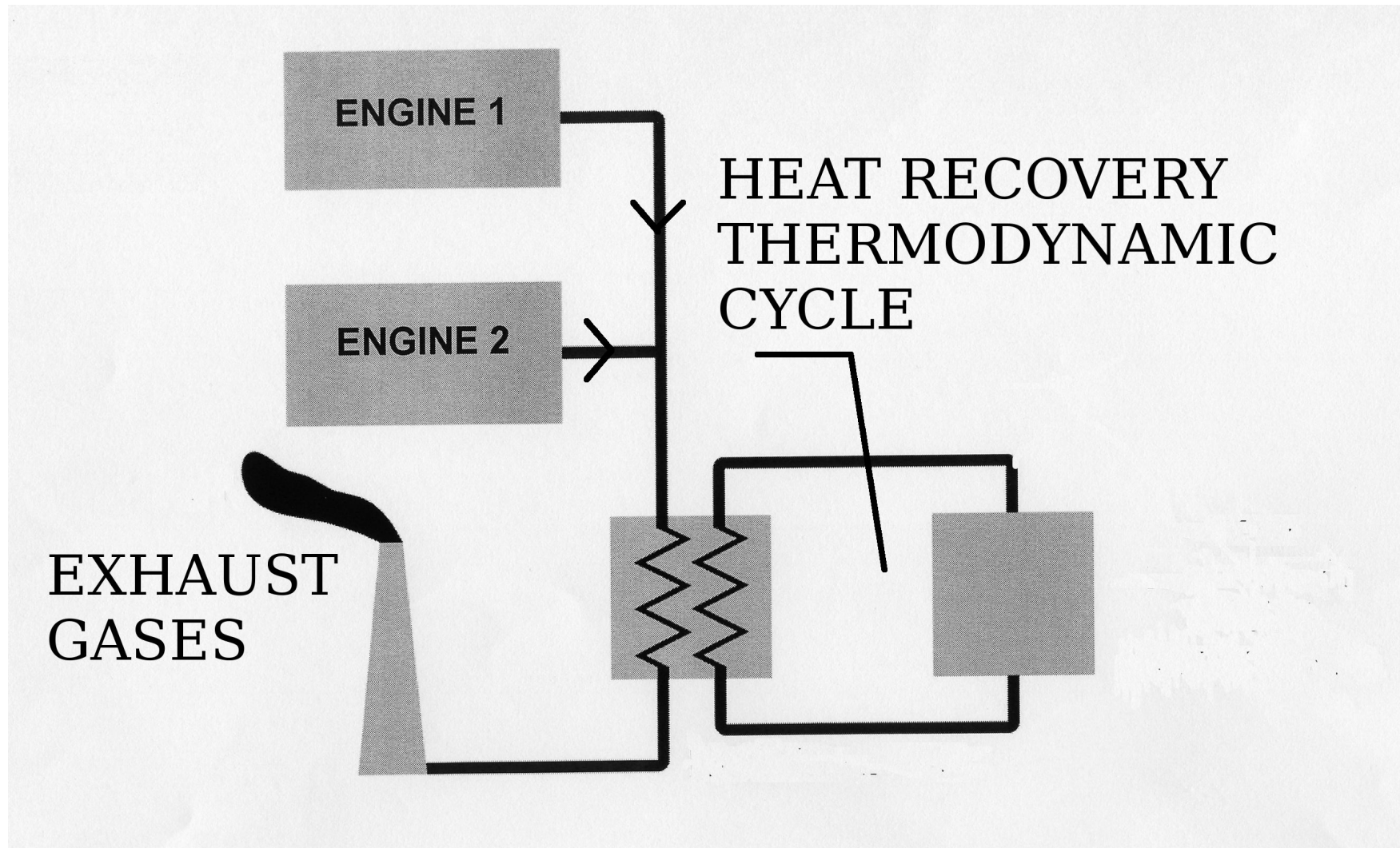


Figure 3

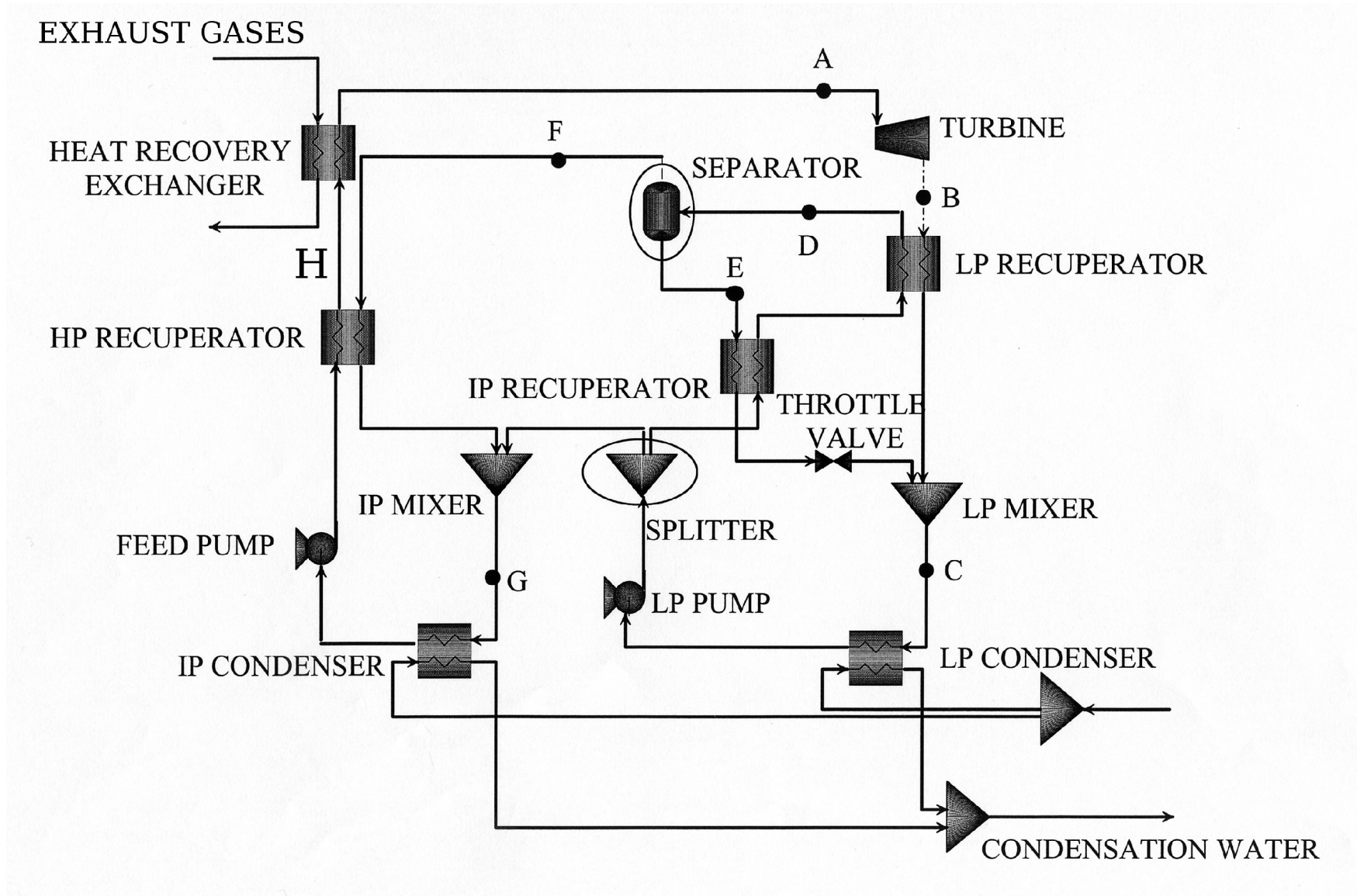


Figure 4.a

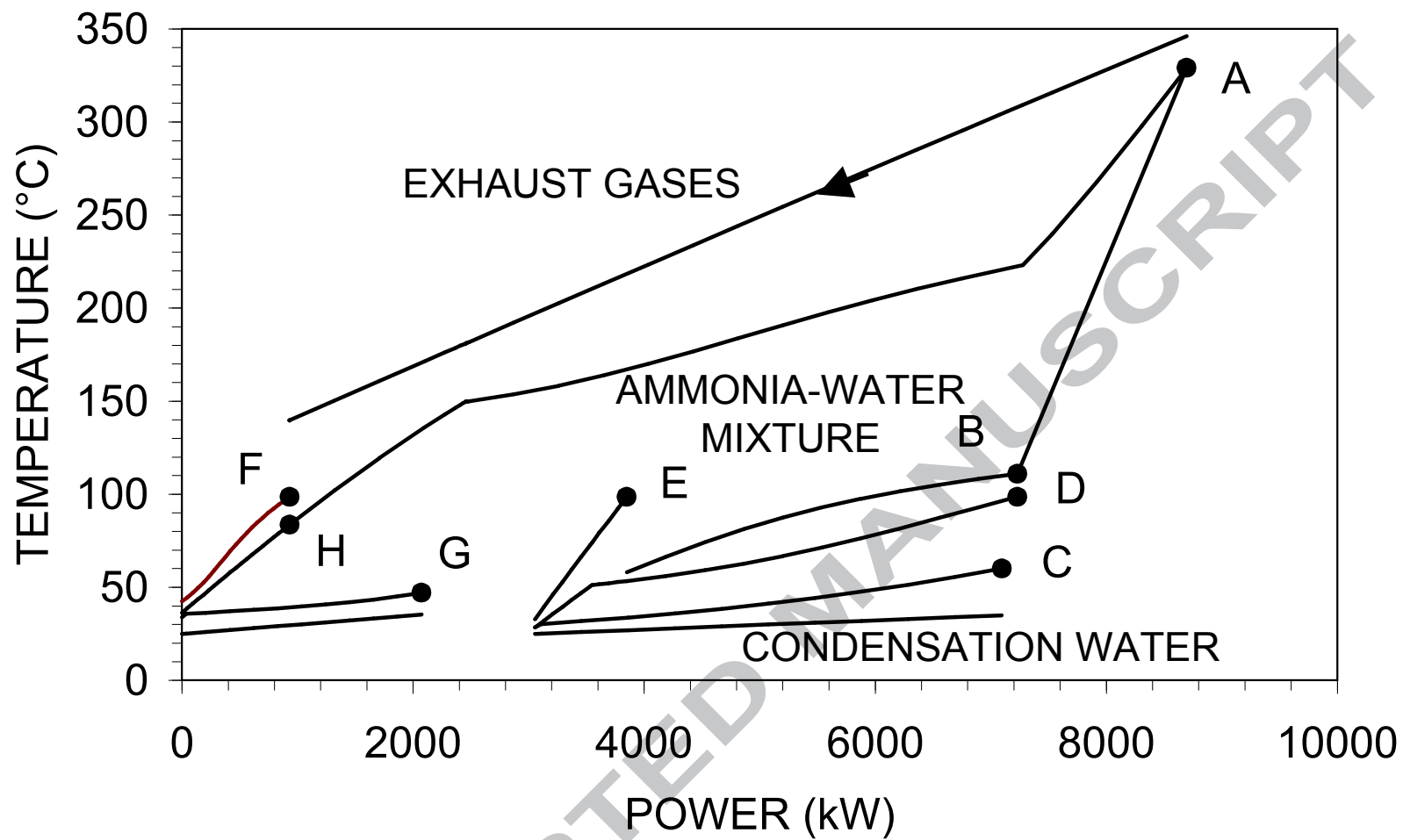


Figure 4.b

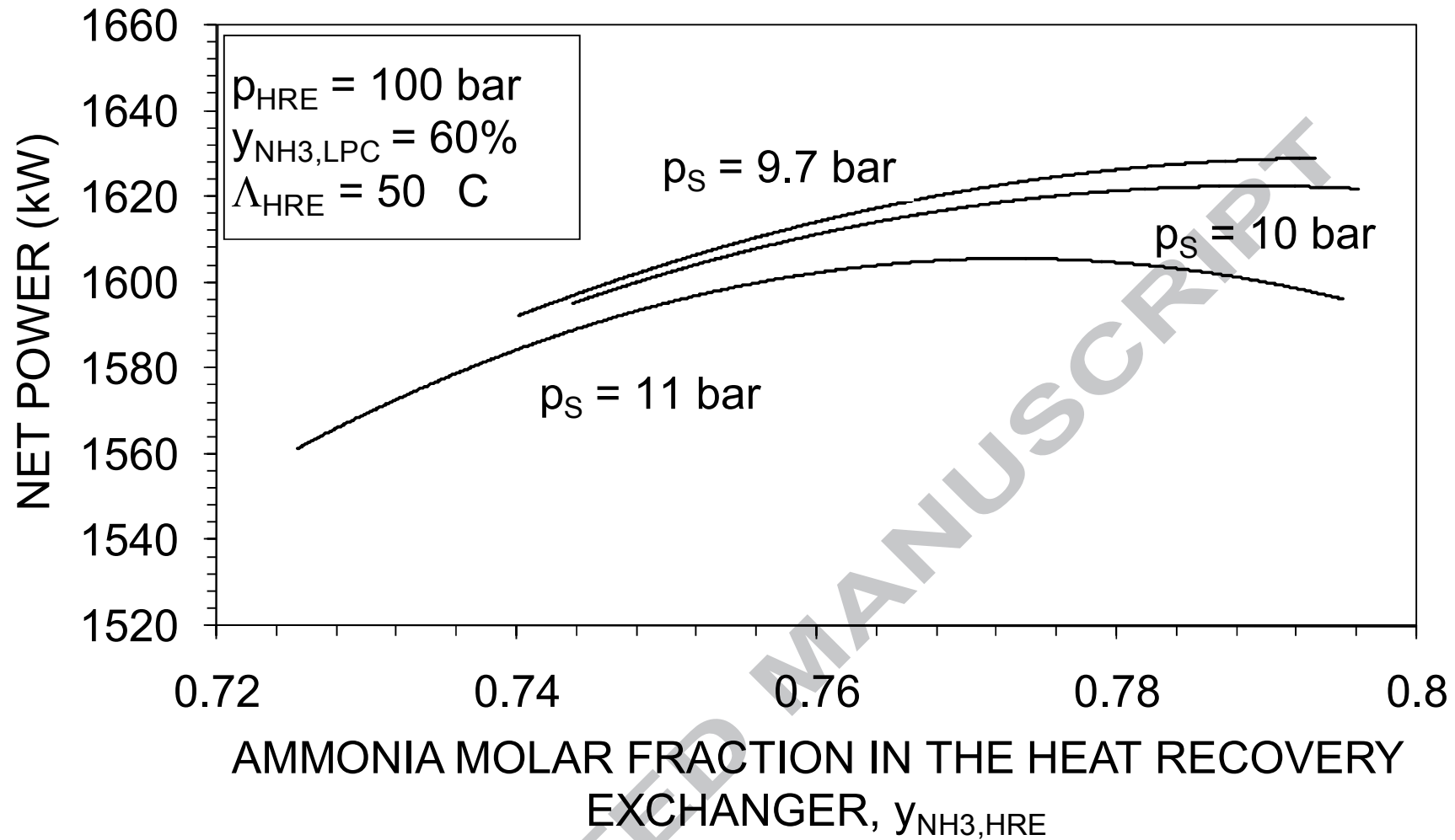


Figure 5

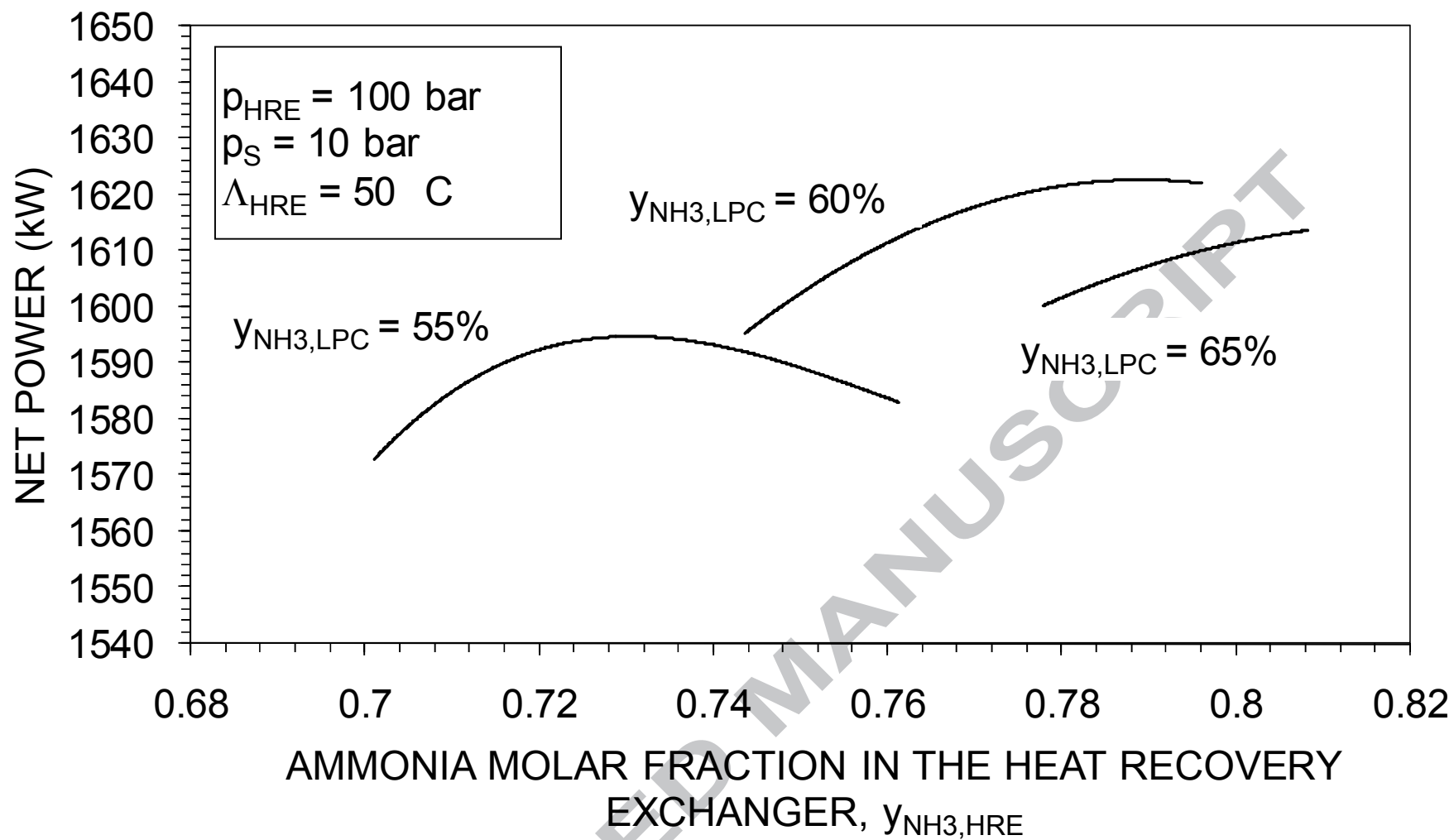


Figure 6

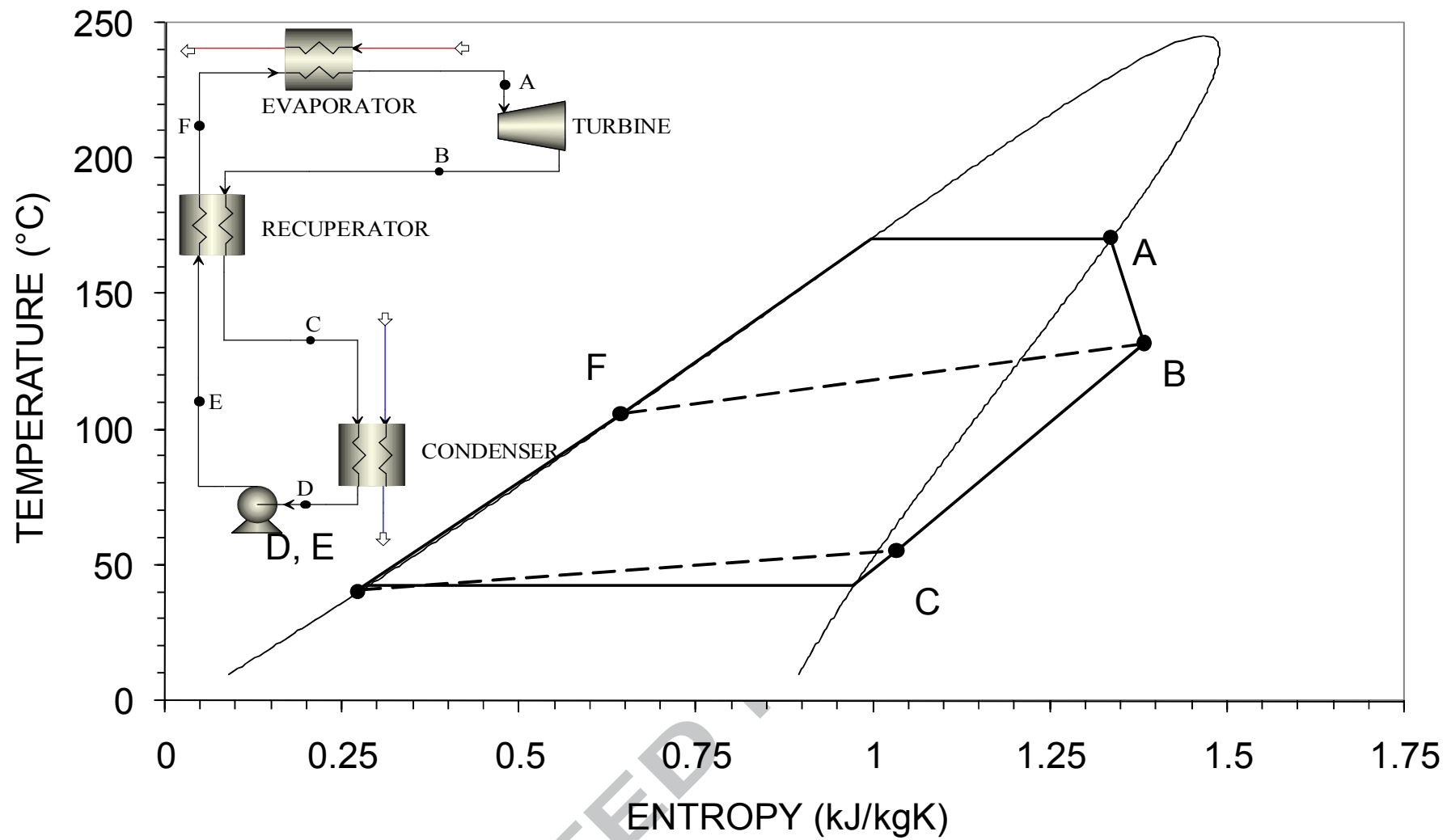


Figure 7

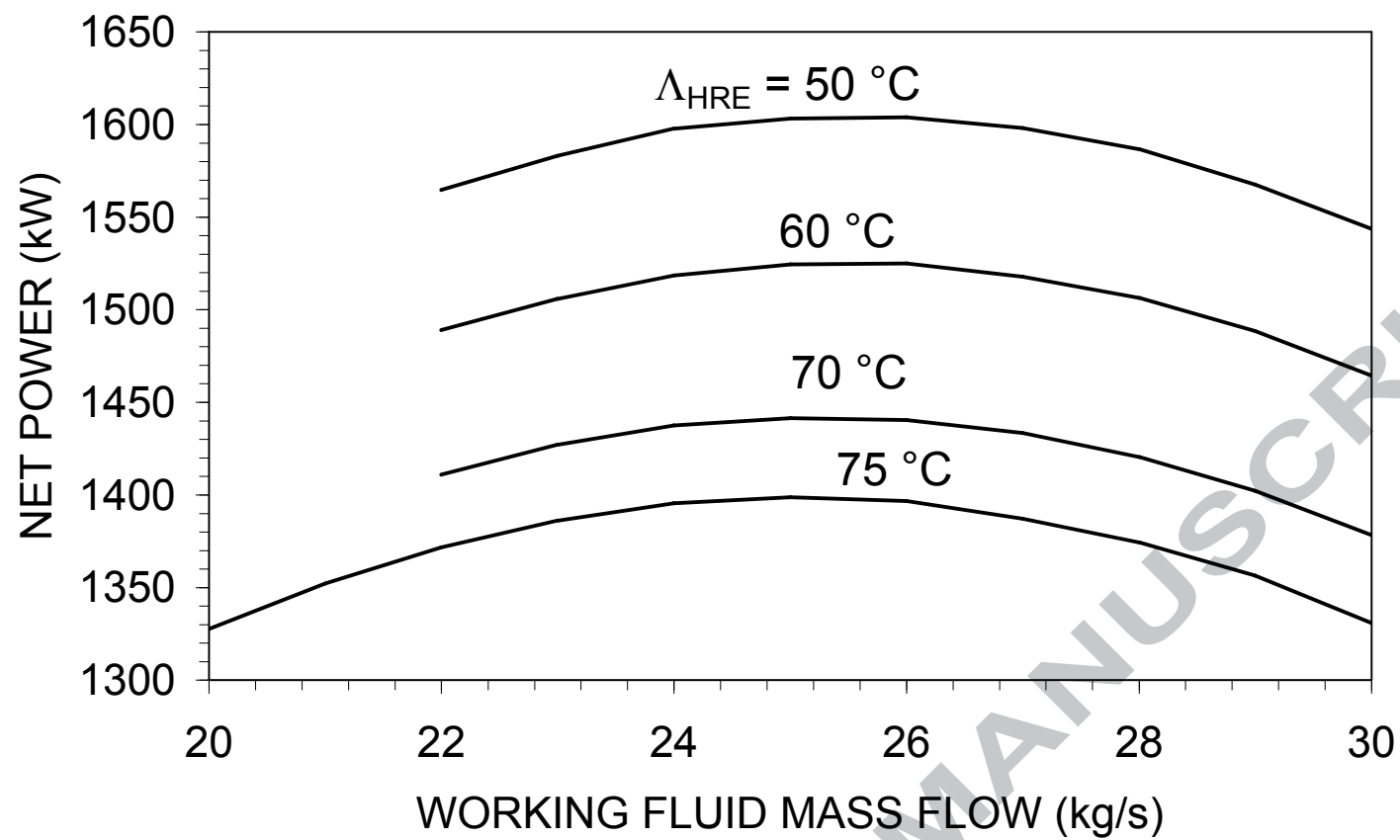


Figure 8

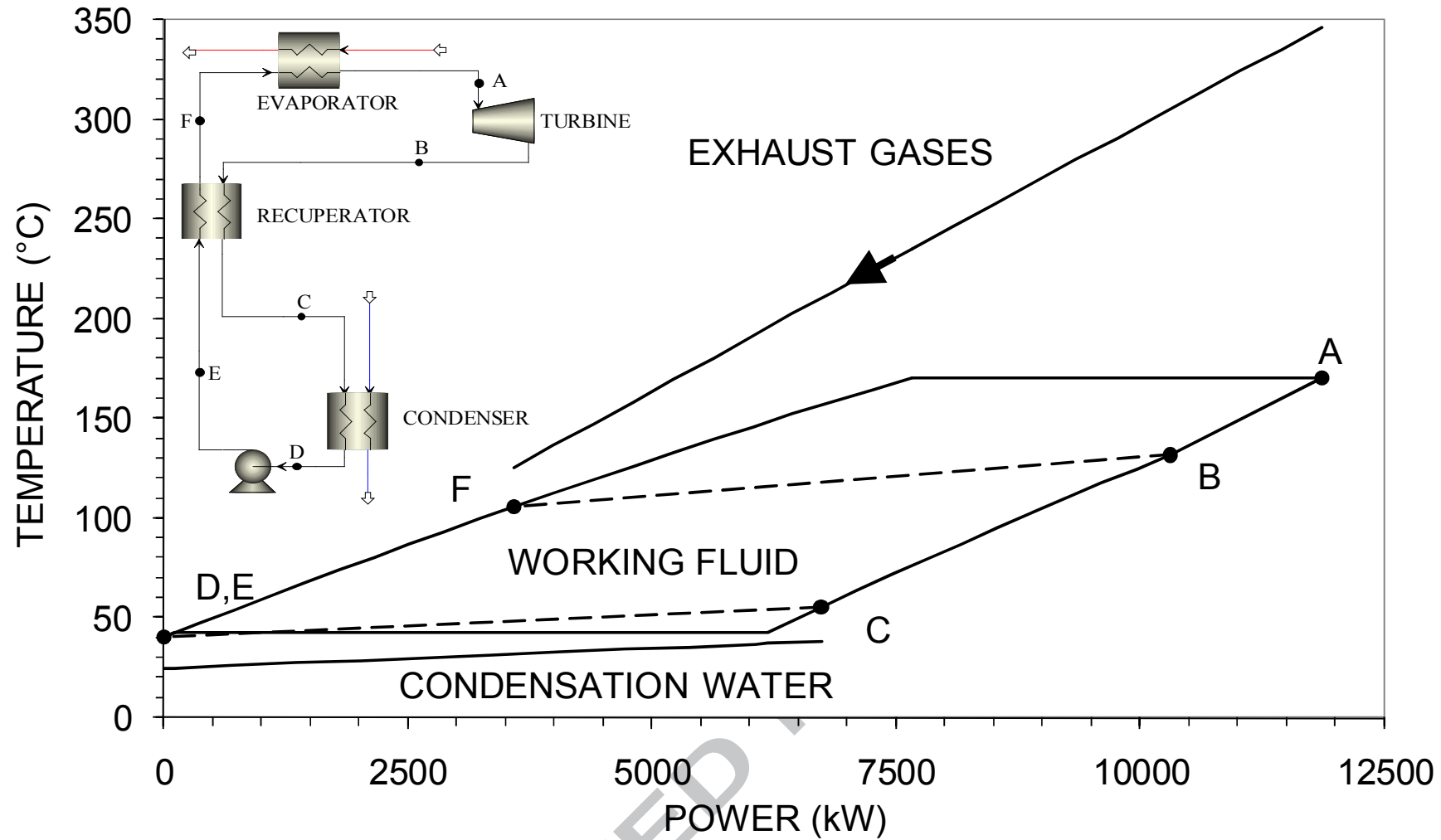
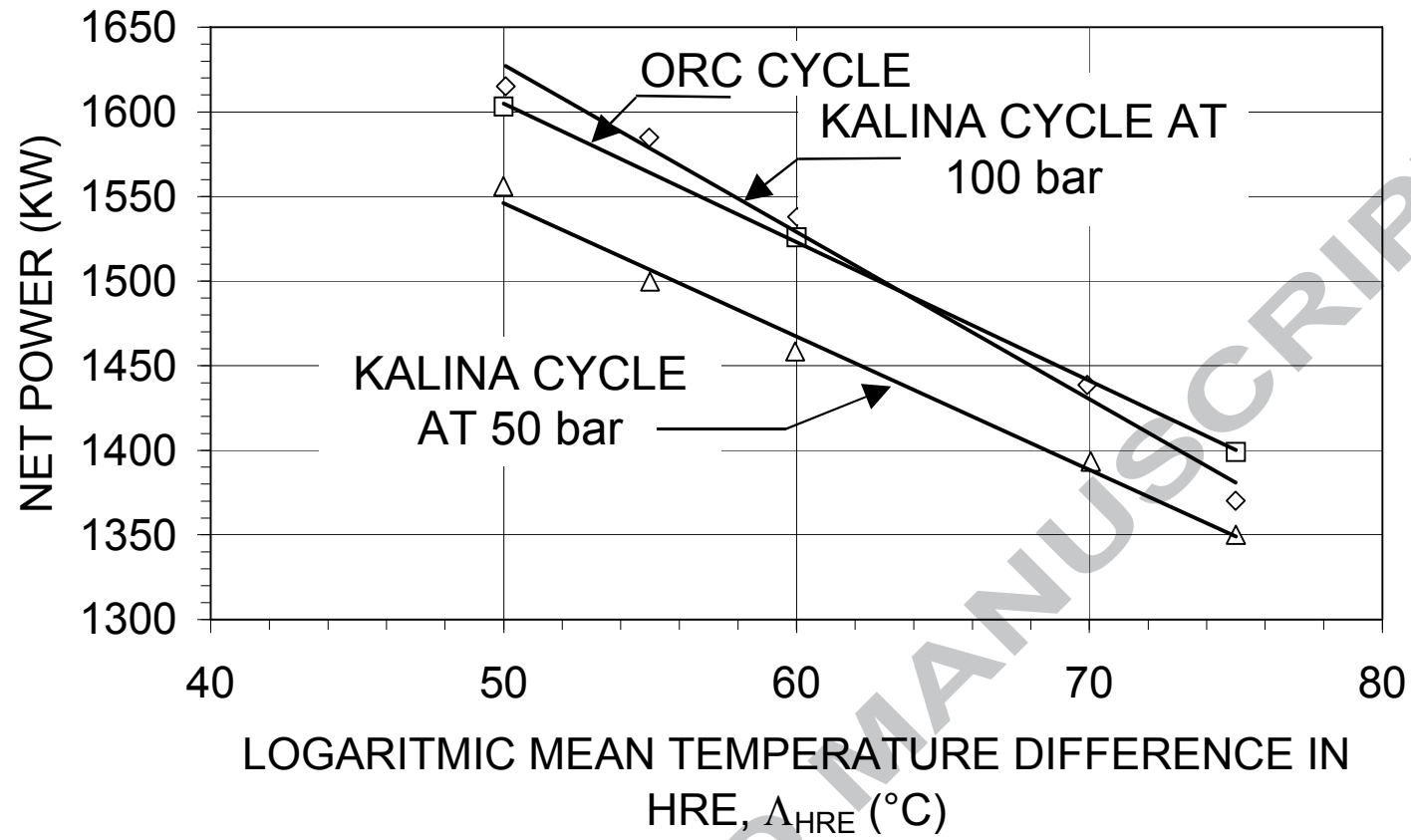


Figure 9

**Figure 10**

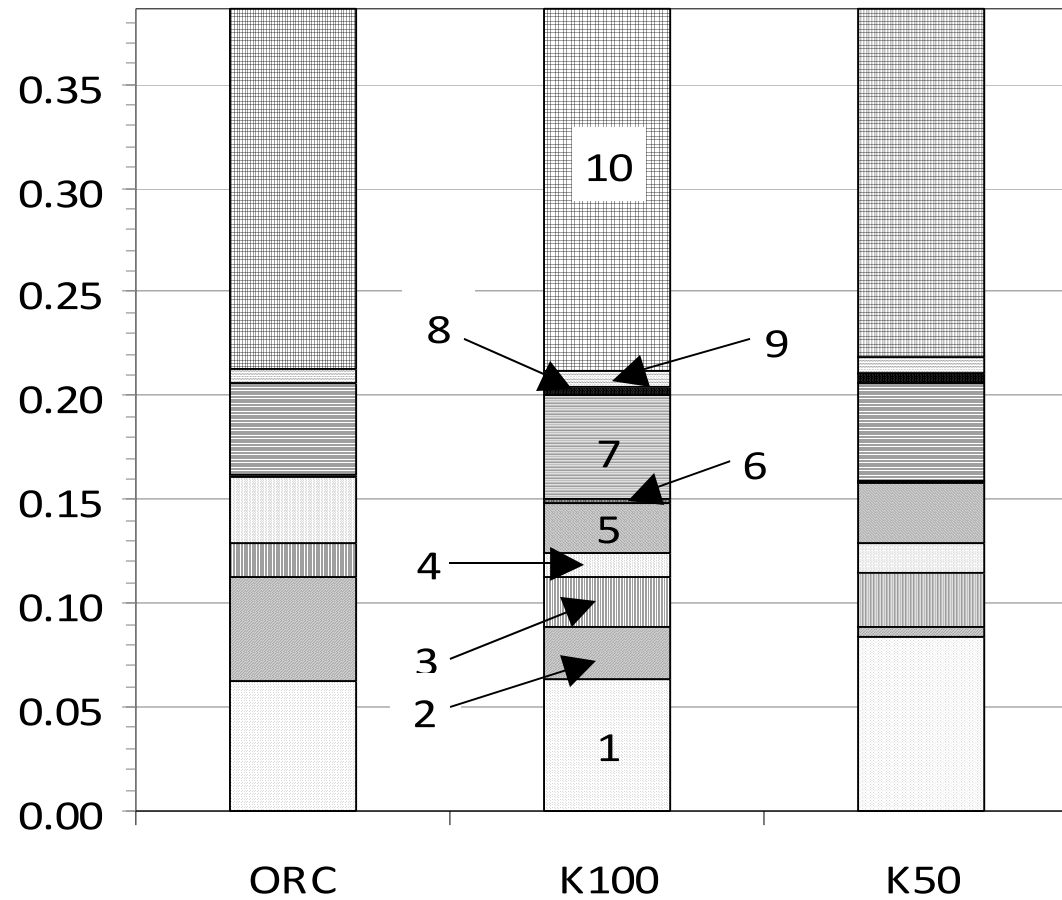


Figure 11